# Toward net-zero sustainable aviation fuel with wet waste–derived volatile fatty acids

Nabila A. Huq[a], Glenn R. Hafenstine[a], Xiangchen Huo[a], Hannah Nguyen[a], Stephen M. Tifft[a], Davis R. Conklin[a], Daniela Stück[a], Jim Stunkel[a], Zhibin Yang[b], Joshua S. Heyne[b], Matthew R. Wiatrowski[a], Yimin Zhang[a], Ling Tao[a], Junqing Zhu[c], Charles S. McEnally[c], Earl D. Christensen[a], Cameron Hays[a], Kurt M. Van Allsburg[a], Kinga A. Unocic[d], Harry M. Meyer III[e], Zia Abdullah[a], and Derek R. Vardon[a,1]

[a]Catalytic Carbon Transformation Center, National Renewable Energy Laboratory, Golden, CO 80401; [b]Mechanical and Aerospace Engineering, University of Dayton, Dayton, OH 45469; [c]Chemical and Environmental Engineering, Yale University, New Haven, CT 06520; [d]Center for Nanophase Materials Sciences, Oak Ridge National Laboratory, Oak Ridge, TN 37380; and [e]Chemical Sciences Division, Oak Ridge National Laboratory, Oak Ridge, TN 37380

Edited by Alexis T. Bell, University of California, Berkeley, CA, and approved February 3, 2021 (received for review November 3, 2020)

**With the increasing demand for net-zero sustainable aviation fuels (SAF), new conversion technologies are needed to process waste feedstocks and meet carbon reduction and cost targets. Wet waste is a low-cost, prevalent feedstock with the energy potential to displace over 20% of US jet fuel consumption; however, its complexity and high moisture typically relegates its use to methane production from anaerobic digestion. To overcome this, methanogenesis can be arrested during fermentation to instead produce $C_2$ to $C_8$ volatile fatty acids (VFA) for catalytic upgrading to SAF. Here, we evaluate the catalytic conversion of food waste–derived VFAs to produce n-paraffin SAF for near-term use as a 10 vol% blend for ASTM "Fast Track" qualification and produce a highly branched, isoparaffin VFA-SAF to increase the renewable blend limit. VFA ketonization models assessed the carbon chain length distributions suitable for each VFA-SAF conversion pathway, and food waste–derived VFA ketonization was demonstrated for >100 h of time on stream at approximately theoretical yield. Fuel property blending models and experimental testing determined normal paraffin VFA-SAF meets 10 vol% fuel specifications for "Fast Track." Synergistic blending with isoparaffin VFA-SAF increased the blend limit to 70 vol% by addressing flashpoint and viscosity constraints, with sooting 34% lower than fossil jet. Techno-economic analysis evaluated the major catalytic process cost-drivers, determining the minimum fuel selling price as a function of VFA production costs. Life cycle analysis determined that if food waste is diverted from landfills to avoid methane emissions, VFA-SAF could enable up to 165% reduction in greenhouse gas emissions relative to fossil jet.**

biojet | food waste | decarbonization | ketonization

Over 21 billion gallons of jet fuel are consumed in the United States annually, with demand expected to double by 2050 (1). The aviation sector accounts for 2.5% of global greenhouse gas emissions, with airlines committing to reduce their carbon footprint by 50% before 2050 (2, 3). Sustainable aviation fuels (SAF) comprise a significant portion of the aviation sector's strategy for $CO_2$ reductions given the limited near-term prospects for electrification (3–5). In addition, the low aromatic content of current SAF routes has been shown to reduce soot formation and aviation-related aerosol emissions by 50 to 70% (2, 6, 7), which can significantly impact the net global warming potential. Soot is the primary nucleator of aviation-induced contrails (8), which have a larger effective radiative forcing (57.4 $mW/m^2$) than aviation-emitted $CO_2$ alone (34.3 $mW/m^2$) (3).

Commercial SAF production in the United States currently relies on the hydrotreating of esters and fatty acids (HEFA) using virgin vegetable oils as well as waste fats, oils, and greases. These feedstocks also serve the renewable diesel market, which in 2018, produced ~300 million gallons of HEFA diesel compared to ~2 million gallons of HEFA SAF (1). Global HEFA capacity is estimated at 1.1 billion gallons per year (BGPY) in 2017 (9). HEFA SAF competes with demand for HEFA diesel, with US fossil diesel consumption estimated at ~47 BGPY (10). Producing HEFA SAF requires an additional catalytic cracking step to convert predominantly $C_{16}$ and $C_{18}$ long chain fatty acids into $C_8$ to $C_{18}$ hydrocarbons suitable for jet fuel. This consumes additional hydrogen and lowers the jet and diesel fuel yield, making HEFA SAF more expensive to produce than HEFA diesel (11). California's Low Carbon Fuel Standard (LCFS) has provided significant economic incentive for producing HEFA from low carbon intensity feedstocks (12), with petroleum companies continuing to retrofit existing refineries (13). Although this expansion will significantly increase biofuel production, the US availability of fats, oils, and greases is capped at ~1.7 BGPY of jet fuel equivalent (14, 15). As such, efforts are needed to develop alternative feedstocks and conversion routes for SAF that avoid direct competition with food resources.

Wet waste is an underutilized feedstock in the United States, with an energy content equivalent to 10.5 BGPY of jet fuel equivalent (assumed 130.4 MJ/gallon). Wet waste includes food

## Significance

To meet the growing demand for sustainable aviation fuels (SAF), conversion pathways are needed that leverage wet waste carbon and meet jet fuel property specifications. Here, we demonstrate SAF production from food waste–derived volatile fatty acids (VFA) by targeting normal paraffins for a near-term path to market and branched isoparaffins to increase the renewable content long term. Combining these distinct paraffin structures was shown to synergistically improve VFA-SAF flash point and viscosity to increase the renewable blend limit to 70%. Life cycle analysis shows the dramatic impact on the carbon footprint if food waste is diverted from landfills to produce VFA-SAF, highlighting the potential to meet jet fuel safety, operability, and environmental goals.

Author contributions: N.A.H., G.R.H., X.H., H.N., S.M.T., J.S.H., M.R.W., Y.Z., L.T., C.S.M., Z.A., and D.R.V. designed research; G.R.H., X.H., H.N., S.M.T., D.R.C., D.S., J.S., Z.Y., M.R.W., Y.Z., J.Z., E.D.C., C.H., K.M.V.A., K.A.U., and H.M.M. performed research; H.N., Z.Y., and J.S.H. contributed new reagents/analytic tools; N.A.H., G.R.H., X.H., H.N., S.M.T., D.R.C., D.S., J.S., Z.Y., M.R.W., Y.Z., L.T., J.Z., E.D.C., C.H., K.M.V.A., K.A.U., H.M.M., and D.R.V. analyzed data; and N.A.H., G.R.H., X.H., H.N., S.M.T., Z.Y., J.S.H., M.R.W., Y.Z., J.Z., C.S.M., K.A.U., and D.R.V. wrote the paper.

Competing interest statement: N.A.H., X.H., H.N., and D.R.V. are inventors on a patent application submitted by the Alliance for Sustainable Energy on methods for the production of VFA-SAF (US 17/121,336 filed on December 14, 2020).

This article is a PNAS Direct Submission.



[1]To whom correspondence may be addressed. Email: derek.vardon@nrel.gov.

This article contains supporting information online at https://www.pnas.org/lookup/suppl/doi:10.1073/pnas.2023008118/-/DCSupplemental.

Published March 15, 2021.

waste (2.5 BPGY), animal manure (4.4 BGPY), wastewater sludge (1.9 BPGY), and the abovementioned waste fats, oils, and grease (1.7 BGPY) (14, 15). While waste lipid feedstocks may be best suited for HEFA refining, valorization strategies are needed for the remaining wet waste feedstocks. Diverting food waste from landfills is of particular note for reducing greenhouse gas emissions, as landfilling one dry ton of food waste has been estimated to release as much as 1.8 tons of $CO_2$ equivalents, assuming landfill methane is collected and recovered for electricity generation (16, 17). Globally, food waste accounts for 6% of greenhouse emissions (18). The high moisture content of wet waste restricts the use of conventional thermochemical conversion approaches (e.g., pyrolysis and gasification) used to produce liquid biofuels from terrestrial biomass, directing technology development efforts toward hydrothermal liquefaction, biological conversion, and hybrid processes (19).

Currently, anaerobic digestion to produce biogas is the leading technology to recover energy from wet waste (20). The high moisture content of wet waste limits its transport and necessitates local processing, with the majority of US anaerobic digestion facilities located near population-dense areas and airports (21). Biogas purification provides a route to pipeline quality renewable natural gas compatible with existing infrastructure. Life cycle analysis has shown that negative carbon intensity can be achieved when producing renewable natural gas from municipal solid waste (−23 g $CO_2$eq/MJ) and dairy waste (−276 g $CO_2$eq/MJ), providing a significant economic driver under the LCFS (12). While renewable natural gas targets an enormous US market (~246 BGPY of jet fuel equivalent) (10), producing liquid hydrocarbon fuels from wet waste offers the potential to address the challenge of decarbonizing the aviation sector.

Anaerobic digestion of wet waste can be arrested prior to methanogenesis to generate both short chain ($C_2$ to $C_5$) and medium chain length ($C_6$ to $C_8$) carboxylic acids as precursors for biofuels and biobased chemicals (14, 22–27), hereon collectively referred to as volatile fatty acids (VFAs). VFA production by arrested methanogenesis offers the potential to utilize existing biogas infrastructure and a wide variety of wet waste feedstocks (14, 22, 28) with ongoing research and development working to increase VFA titers, rates, and yields by tailoring feedstock composition, microbial consortia, fermentation parameters, and online separation technologies (14, 22, 29–31). Currently, $C_2$ to $C_5$ carboxylic acids are primarily produced from the oxidation of petroleum derivatives, while $C_6$ and $C_8$ carboxylic acids are primarily derived from coconut and palm oil (29). Propionic acid ($C_3$) and butyric acid ($C_4$) address chemical market volumes on the order of 0.1 to 0.2 BGPY (29), while medium chain length carboxylic acids target smaller specialty markets. Given the availability of wet waste and potential saturation of biobased chemical markets in the long term, VFAs provide a potential target intermediate for catalytic upgrading into low carbon intensity biofuel (23, 25, 26, 32–35).

VFAs can be catalytically upgraded to SAF through carbon coupling and deoxygenation chemistries. Depending on their chain length, VFAs can be converted into normal paraffins identical to those found in petroleum or undergo an additional carbon coupling step to generate isoparaffin, cycloparaffin, and aromatic hydrocarbons with molecular structures distinct from fossil jet (Fig. 1).

Ketonization is the first unit operation to elongate the carbon backbone of VFAs (14, 22). Ketonization reacts two VFAs to produce a single ketone that is one carbon shorter than the sum of both acids and removes oxygen in the form of water and carbon dioxide (36, 37). Ketonization of acetic acid to acetone has been commercialized (37), with longer chain acids actively researched for biofuel and biochemical applications. Following ketonization, ketones $\geq C_8$ can undergo direct hydrodeoxygenation (Fig. 1, *Top*) to produce normal paraffin-rich hydrocarbons. In comparison, ketones $\leq C_7$ require a second carbon coupling step prior to hydrodeoxygenation to fall within the $C_8$ to $C_{18}$ range of jet fuel (Fig. 1, *Bottom*). Ketone carbon coupling can take place by various pathways including aldol condensation chemistry (25) as well as ketone reduction to alcohols for further dehydration and oligomerization (32, 34). Aldol condensation of central ketones is an emerging bench-scale chemistry that can generate structurally unique isoparaffins (38) with significantly lower freezing points for jet fuel applications due to the high degree of branching as well as reduce the intrinsic sooting tendency relative to aromatic hydrocarbons by over twofold (25).

Normal paraffins produced from VFAs (Fig. 1, *Top*) can provide fungible hydrocarbons identical to those in petroleum that offer a near-term path to SAF qualification and market entry. In the United States, new SAF conversion routes must complete a rigorous qualification process to ensure fuel safety and operability overseen by ASTM International, the Federal Aviation Administration, and aviation original equipment manufacturers (OEMs). There are currently seven ASTM-approved routes for SAF that are derived from Fischer–Tropsch processing of syngas, the abovementioned esters and fatty acids, farnesene, ethanol, isobutanol, and algal hydrocarbons (39). Further details summarizing current ASTM-qualified routes to SAF can be found in *SI Appendix*, Table S1. Historically, ASTM qualification can require jet fuel volumes on order of over 100,000 gallons in order to pass a four-tiered screening process and two OEM review stage gates that may take place over a period of 3 to

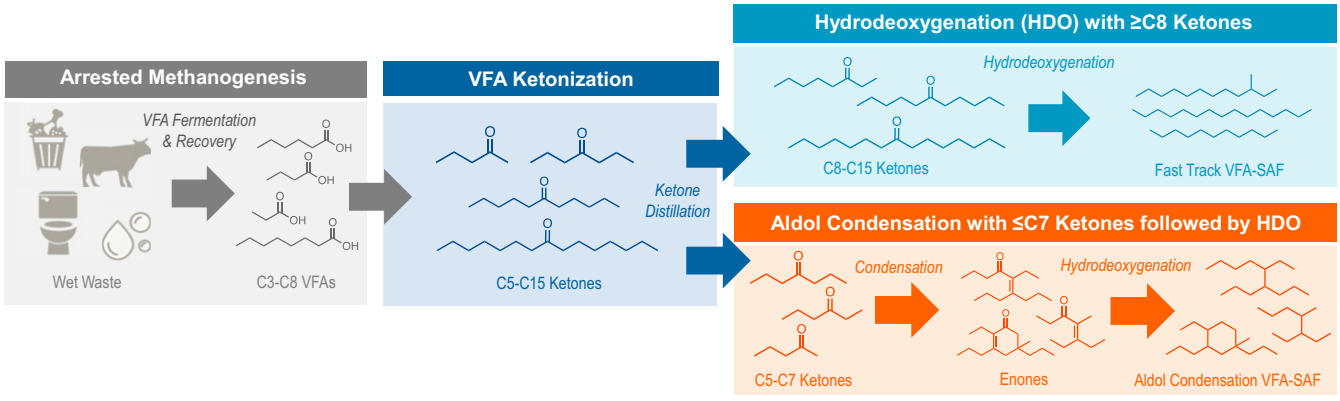


**Fig. 1.** Overview scheme of the major oxygenate and hydrocarbon molecules produced when converting wet waste VFA into Fast Track VFA-SAF that is composed of normal paraffin-rich hydrocarbons (*Top Right*) and Aldol Condensation VFA-SAF composed of isoparaffin-rich hydrocarbons (*Bottom Right*).

7 y (40). To help reduce this barrier, in January 2020, ASTM approved a new "Fast Track" qualification process for SAF routes that produce hydrocarbons structurally comparable to those in petroleum jet with a 10 vol% blend limit (41). "Fast Track" eliminates two tiers of testing and facilitates approval with under 1,000 gallons of fuel and within the timeframe of 1 to 2 y (42).

In contrast, isoparaffins derived from aldol condensation can offer complementary fuel properties to increase the renewable blend content of VFA-SAF blends, but the unique chemical structures would not qualify for "Fast Track" approval. To accelerate the approval of SAF routes that produce molecules distinct from petroleum jet, small-volume fuel tests and predictive tools are being developed for the most critical bulk properties, which screen for potentially deleterious engine operability effects (i.e., lean blowout, cold ignition, and altitude relight) (43). These tests, referred to as Tier α and β prescreening (44), evaluate SAF candidates for established ASTM D7566 properties, as well as novel properties observed to be important through the National Jet Fuels Combustion Program (*SI Appendix*, Table S2) (43). New properties include surface tension and derived cetane number (CN), which impact ignition and lean blowout propensity, respectively. At less than one mL of test volume, Tier α can utilize gas chromatograph (GC) and GCxGC method data to predict all critical properties. With between 50 and 150 mL of neat material (depending on the CN measurement method used), Tier β test methods can measure the critical unblended operability properties. In terms of emissions, low-volume sooting tendency measurement methods have been developed that require <1 mL of fuel versus the 10 mL required to measure smoke point (45, 46). Combined, these new methods allow for rapid evaluation of developing SAF conversion routes.

To advance the technology and fuel readiness level of VFA-SAF, this work evaluates the production of drop-in normal paraffins and structurally unique isoparaffins from food waste–derived VFAs. First, VFAs were biologically produced from food waste and recovered neat by an industry partner, Earth Energy Renewables. A simplified kinetic model was then developed for mixed VFA ketonization to determine the ketone carbon chain length distribution suitable for SAF production by each conversion route, with model results compared to experiments with biogenic VFAs. VFA ketonization was assessed for >100 h of continuous time-on-stream (TOS), with trace impurities characterized within the incoming biogenic VFA feed. Catalyst regeneration was evaluated for coke and impurity removal, as well as to compare fresh and regenerated catalyst activity. Following VFA ketonization, $\geq C_8$ ketones were processed by direct hydrodeoxygenation to generate predominantly normal paraffins suitable for 10% blend testing for ASTM Fast Track, hereon referred to as "Fast Track VFA-SAF." In parallel, VFA-derived ketones $\leq C_7$ were processed via aldol condensation and hydrodeoxygenation to produce predominantly isoparaffin hydrocarbons for Tier α and Tier β prescreening, hereon referred to as "Aldol Condensation VFA-SAF." Higher blends with both VFA-SAF fractions were examined to increase the renewable carbon content and reduce soot formation while still meeting fuel property specifications. Lastly, techno-economic and life cycle analysis was performed to evaluate the sensitivity of catalytic process parameters on VFA-SAF production costs as well as potential greenhouse gas reductions relative to fossil jet.

## Results and Discussion

**Food Waste–Derived VFAs.** Mixed VFAs were produced neat (<3% water) by pilot-scale anaerobic digestion of food waste via arrested methanogenesis with integrated online separation by an industry partner, Earth Energy Renewables. VFA chain lengths ranging from $C_3$ to $C_8$ were recovered in their neat acid form without salt formation, while acetic acid was recycled for chain elongation during fermentation. Additional details on VFA production are provided in *SI Appendix*, section S1 and Table S3. Two VFA samples comprised predominantly of $C_6/C_8$ and $C_4/C_6$ VFA were initially prepared for downstream catalytic upgrading (Fig. 2 *A* and *D*). Minimal impurity levels were observed by elemental analysis, with only K, Na, N, and S measured above 10 ppm (Table 1).

**VFA Ketonization Model.** A simplified kinetic model was developed and used to evaluate carbon flow to the suitable ketone upgrading pathways based on the incoming VFA chain length distribution, as shown in Fig. 2 *A* and *D*. Both the $C_6/C_8$ and $C_4/C_6$ VFA sample carbon chain length distributions were modeled by accounting for higher rates of cross-ketonization relative to self-ketonization (47). Model results were then compared against ketone profiles determined experimentally under complete conversion conditions (Fig. 2 *C* and *F* and *SI Appendix*, Figs. S1–S3).

Modeled ketone chain length distributions were in good agreement with experimental results, with <10% difference in the mole fraction for a given carbon number. The $C_6/C_8$ VFA sample yielded a majority of ketones with chain lengths $\geq C_8$ suitable for direct hydrodeoxygenation for the Fast Track VFA-SAF conversion pathway (95% modeled and 95% experimental). In comparison, slightly less than half of the ketones produced from the $C_4/C_6$ VFA sample were $\geq C_8$ (47% modeled and 44% experimental), with a near equal portion $\leq C_7$ suitable for the Aldol Condensation VFA-SAF conversion pathway. To demonstrate the robustness of this model, an additional VFA profile was experimentally tested and shown to be in close agreement with the predictive ketone carbon number distribution model (*SI Appendix*, Fig. S2).

**Ketonization Catalyst Performance.** The stability of a commercial $ZrO_2$ catalyst for ketonization was evaluated with both model and biogenic VFAs derived from food waste. Previous studies by our team have shown full conversion of butyric acid with near theoretical ketone yield using this catalyst (25); therefore, partial conversion conditions were evaluated with mixed model VFAs reflective of the $C_4/C_6$ profile to assess stability with 72 h of TOS (*SI Appendix*, Fig. S4). The first 48 h of TOS resulted in 6% drop in conversion which appeared to stabilize with the final 24 h showing only 2% drop in conversion. This suggests carbon laydown may initially occur on strong acid sites (48) which may be manageable with periodic oxidative regeneration.

Complete and partial conversion runs were then performed with biogenic VFAs to assess the deposition of biogenic impurities and regenerability of the catalyst. The biogenic VFA feed contained trace alkali impurities, as well as sulfur (Table 1), which may deposit on the catalyst surface and poison acid sites over time, particularly alkali elements that are known to deactivate reducible metal oxides (49, 50). The complete conversion run was performed for over 100 h of TOS with the $C_6/C_8$ VFA sample (Fig. 3*A*). Analysis of the spent $ZrO_2$ by X-ray photoelectron spectroscopy (XPS) (Fig. 3*B* and *SI Appendix*, Table S4) and scanning transmission electron spectroscopy in conjunction with energy dispersive X-ray spectroscopy (STEM-EDS) (*SI Appendix*, Fig. S5) showed no measurable levels of biogenic impurities on the catalyst surface, within the limits of detection. Analysis of the self-separating ketonization organic phase showed impurity levels at or below ppm detection limits (Table 1) which suggests partitioning of impurities into the aqueous phase as confirmed in *SI Appendix*, Table S5. Thermal gravimetric analysis (TGA) of the spent catalyst measured a carbon content of 1.8 wt% (Table 2) that was confirmed by CHN (carbon, hydrogen, and nitrogen) analysis (C 1.6 wt%), which may be due to the formation of larger oligomers from ketone condensation that deposit on the surface. Surface area and total pore

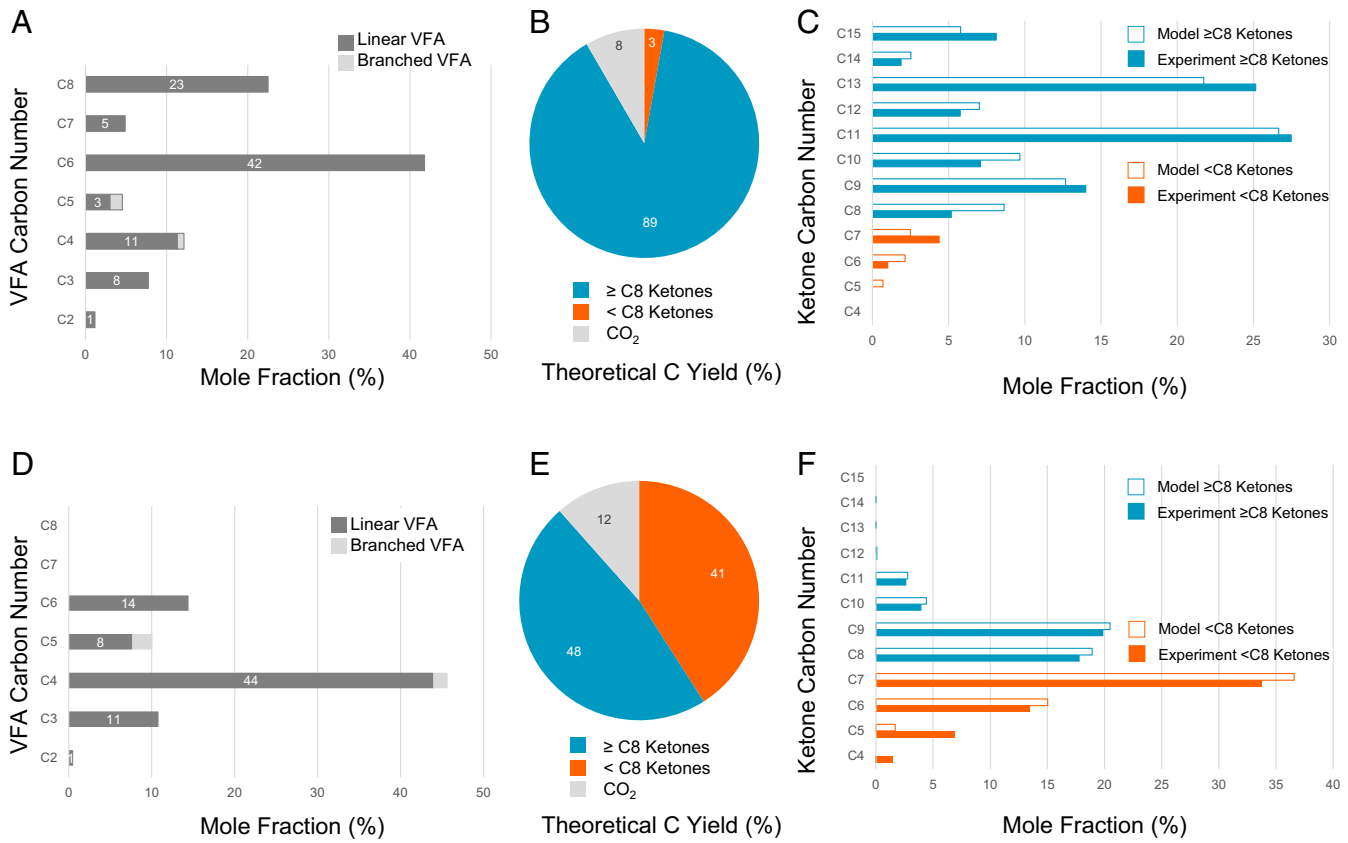


**Fig. 2.** Modeled and experimental VFA ketonization carbon yields. For the $C_6/C_8$ VFA feed, (*A*) VFA carbon chain length distribution, (*B*) ketone and $CO_2$ carbon yield, and (*C*) model and experimental ketone carbon number profile. Similar values are reported for the $C_4/C_6$ VFA feed (*D*–*F*). Blue represents $\geq C_8$ ketone carbon chain lengths suitable for Fast Track VFA-SAF, while orange represents $\leq C_7$ ketones that require coupling for Aldol Condensation VFA-SAF. Values are rounded to whole number.

volume decreased by <10%, consistent with the relatively low coke content.

Regeneration of the 100-h spent $ZrO_2$ catalyst exposed to biogenic impurities was performed by a typical oxidation cycle in flowing air at 500 °C. Following regeneration, carbon was no longer detected on the catalyst surface by TGA. and similar textural properties and surface acidity were observed as the fresh catalyst (Table 2 and *SI Appendix*, Figs. S6 and S7). Ketonization partial conversion tests (~37% VFA conversion, 290 °C, weight hourly space velocity of 7.7 $h^{-1}$) confirmed comparable ketonization activity between the fresh and regenerated catalyst using the biogenic $C_4/C_6$ VFA sample with online detection of effluent gas $CO_2$ by nondispersive infrared detection (NDIR), with differences within experimental error (Fig. 3*C*). Analysis of the liquid products are also provided in *SI Appendix*, Fig. S8. As anticipated based on the spent catalyst characterization results, impurities

**Table 1. Elemental analysis of the feed and upgrading products for $C_4/C_6$ and $C_6/C_8$ food waste–derived VFA samples**

| ppm | Neat VFA $C_4/C_6$ | Neat ketone $C_4/C_6$ | Fast Track VFA-SAF $C_4/C_6$ | Neat VFA $C_6/C_8$ | Neat ketone $C_6/C_8$ | Fast Track VFA-SAF $C_6/C_8$ |
|---|---|---|---|---|---|---|
| Al | <0.4 | <0.4 | <0.4 | 1.2 | <1 | <0.4 |
| B | <0.2 | <0.2 | <0.2 | 1.8 | <1 | <0.2 |
| Ca | <0.1 | <0.1 | <0.1 | 0.8 | <0.1 | <0.1 |
| Fe | 0.4 | <1 | <1 | 3.0 | <0.1 | <0.1 |
| K | <1 | <1 | <1 | 236 | <1 | <1 |
| Mg | <0.1 | <0.1 | <0.1 | 4.1 | <0.1 | <0.1 |
| Mn | <0.1 | <0.1 | <0.1 | <0.2 | <0.2 | <0.1 |
| N | 37.0 | ND | 1.2 | 67.7 | 25.9 | ND |
| Na | 11.8 | <1 | <1 | 104.8 | <1 | <1 |
| P | <1 | <1 | <1 | <10 | <10 | <1 |
| S | 8.2 | 1.0 | <1 | 32 | <10 | <1 |
| Si | <1 | <1 | <1 | <1 | <1 | <1 |
| Zn | <0.1 | <1 | <0.1 | <1 | <1 | <0.1 |

ND: not determined due to volume limitations.

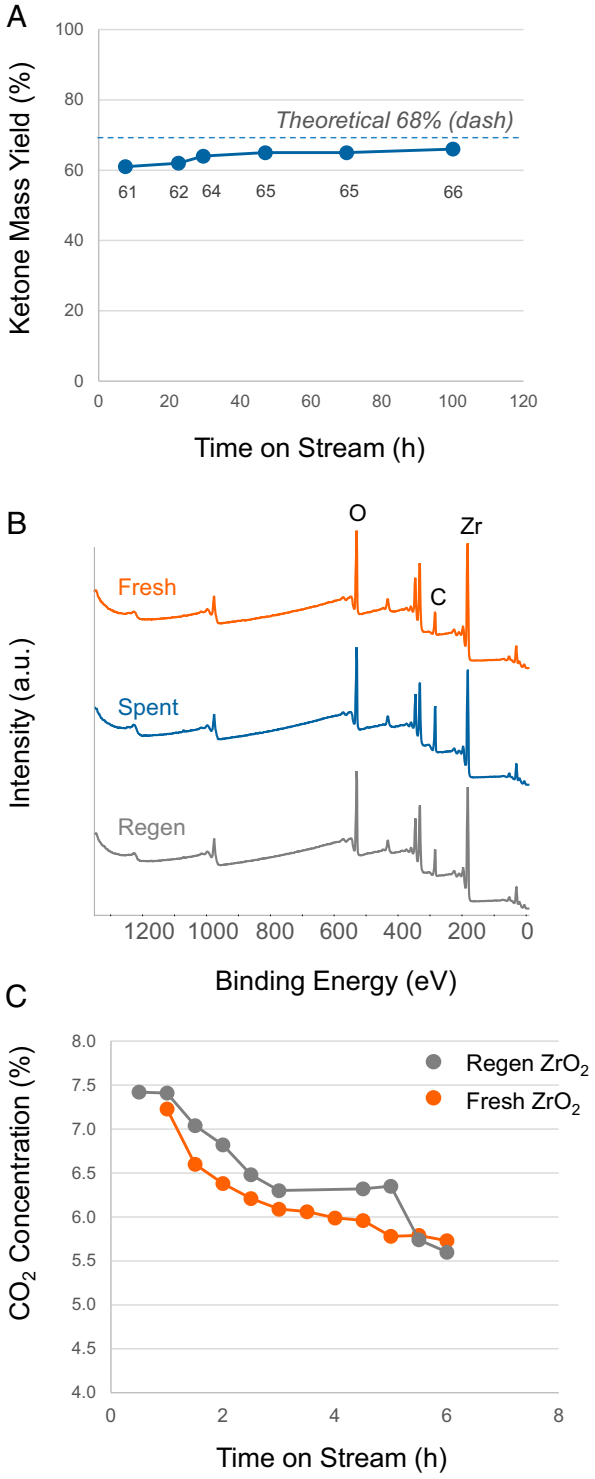


**Fig. 3.** Ketonization catalyst performance with the biogenic $C_6/C_8$ VFA sample. (*A*) Complete conversion conditions with near theoretical yields. Reaction conditions: catalyst loading 5 g $ZrO_2$, Ar flow 166 mL(STP)/min$^{-1}$ at 1 atm, bed temperature 350 °C, and weight hourly space velocity (WHSV) 3.1 h$^{-1}$ based on VFA mass flow rate. (*B*) XPS survey spectra of fresh, spent, and regenerated $ZrO_2$. (*C*) Ketonization catalyst stability under partial conversion conditions before and after regeneration using the spent full conversion catalyst. Reaction conditions: catalyst loading 2 g $ZrO_2$, Ar flow 166 mL(STP)/min$^{-1}$ at 1 atm, bed temperature 290 °C, and WHSV 7.7 h$^{-1}$ based on VFA mass flow rate. Regeneration conditions: 5 °C/min to 500 °C, hold 12 h, cool naturally, and in flowing air.

were not detected on the regenerated $ZrO_2$ (Fig. 3*B* and *SI Appendix*, Table S4 and Fig. S5) with comparable crystallite sizes before and after oxidative treatment (*SI Appendix*, Fig. S9). Future work is planned to decouple the impacts of carbon laydown and biogenic impurities as a function of catalyst surface acidity, VFA chain length, and process conditions over prolonged TOS.

**Fast Track VFA-SAF.** Ketones derived from the $C_6/C_8$ VFA sample were processed directly by hydrodeoxygenation to produce predominantly normal paraffins suitable for Fast Track VFA-SAF. Hydrodeoxygenation was performed with a 3% $Pt/Al_2O_3$ catalyst prepared in house and studied in previous work (25). Hydrocarbon production was observed for up to 48 h of TOS under complete conversion conditions with a liquid mass balance of 99% (*SI Appendix*, Fig. S10). It should be noted that partial conversion studies are needed to evaluate hydrodeoxygenation catalyst stability with biogenic ketones in regard to both carbon laydown and impurity deactivation. This effort is ongoing by our team and beyond the scope of this initial study. Following hydrodeoxygenation, the hydrocarbon phase was decanted, and trace amounts of $<C_7$ hydrocarbons ($\leq$9.8% of sample mass) were removed by distillation prior to neat and blended fuel property analysis. The overall VFA-to-hydrocarbon carbon yield was 79% (mass yield 58%) which approached theoretical (82% carbon yield and 61% mass yield).

Neat fuel properties of Fast Track VFA-SAF produced from the $C_6/C_8$ VFA sample were then evaluated by Tier α and β screening (44) (*SI Appendix*, Table S2). Values were compared to specifications for an aviation fuel containing SAF as defined by ASTM D7566 Table 1 and are shown visually in Fig. 4 against gray regions representing representative fossil jet properties (51). The neat Fast Track VFA-SAF displayed an average carbon number of 11.3 (Fig. 4*A*) which was comparable to the average value of commercial Jet A of 11.4 (*SI Appendix*, Table S6). The VFA-SAF sample was predominantly normal paraffins, with 7 wt % isoparaffins and 2 wt% cycloparaffins detected. Fuel property measurements of the neat sample (*SI Appendix*, Tables S7 and S8) confirmed its moderately higher net heat of combustion (nHOC) than the reference fossil jet fuel (43.4 MJ/kg, Jet A 43.0 MJ/kg), with viscosity and surface tension being within the typical range of fossil jet. Normalized sooting concentration measurement for a 20 vol% blend (0.87) suggests that neat Fast Track VFA-SAF extrapolates to a 65% reduction in sooting relative to fossil Jet A (*SI Appendix*, Table S8). However, the high concentration of small ($\leq C_9$) normal paraffins resulted in flash point being below specifications (31 °C, spec 38 °C), gravimetric density being below specifications (743 kg/m$^3$, spec 775 to 840 kg/m$^3$), and boiling point distribution being below the typical range for Jet A (*SI Appendix*, Table S8). The limited degree of molecular branching also resulted in freezing point above spec (−27 °C, spec −40 °C).

To address neat fuel property limitations, Fast Track VFA-SAF was blended at 10 vol% with Jet A. Blending at 10 vol% resulted in all measured fuel properties being within spec (Table 3 and Fig. 4 *A*–*C*). The freezing point of neat Jet A increased by 5 °C to −47 °C upon blending, staying well below the limit of −40 °C. No change was observed in the flash point of Jet A after blending due to the low concentration of volatile components. The boiling point distribution of the blend was within the typical range of fossil jet fuel (Fig. 4*C*). Improvements in neat Jet A fuel properties upon blending included a modest increase in specific energy density to 43.2 MJ/kg, an increase in the indicated cetane number from 48 to 52, and based on the 20 vol% measurement (*SI Appendix*, Table S8), an anticipated decrease of 6.5% in normalized soot concentration. Additionally, the acidity of the blend is anticipated to be 0.02 mg KOH/g (based on the measured 0.15 mg KOH/g acidity of the neat fuel) which is well within the blend maximum of 0.10 mg KOH/g. While Fast Track

**Table 2. Fresh, spent, and regenerated $ZrO_2$ catalyst material properties used for 100 h of continuous time on stream ketonization of the $C_6/C_8$ VFA sample (Fig. 2)**

| $ZrO_2$ catalyst sample | Surface area ($m^2$/g) | Pore volume (mL/g) | Total acidity (μmol/g) | Carbon content (wt%) |
|---|---|---|---|---|
| Fresh | 51.3 | 0.29 | 246 | NA |
| 100 h spent | 47.6 | 0.27 | ND | 1.8 |
| Regenerated | 48.4 | 0.30 | 233 | 0.0 |

NA: not applicable for fresh catalyst. ND: not determined due to carbon laydown that interferes with measurement.

limits blending to 10 vol%, additional testing determined that the 20 vol% blend still met flashpoint criteria (*SI Appendix*, Tables S8 and S9).

**Aldol Condensation VFA-SAF.** Highly branched isoparaffins produced from Aldol Condensation VFA-SAF were then evaluated for their neat and blended Tier α and Tier β fuel properties. Batch aldol condensation reactions were performed with the $<C_8$ ketones derived from the $C_4/C_6$ VFA sample. Ketones $<C_8$ were initially separated by fractional distillation and condensed in a batch reactor. The ketones were prepared at 20 wt% in decane as an appropriate boiling point solvent that also facilitated tracking ketone conversion by GC. $Nb_2O_5$ powder catalyst was selected due to its high acidity and activity for internal ketone condensation. Recent work has shown internal ketones are an order of magnitude less reactive than terminal ketones and require highly acidic metal oxides (25, 52). Single-pass ketone conversion to enones was dependent on molecular structure, varying between 12 and 100% (*SI Appendix*, Table S10). Ketone condensation can also form cyclic and aromatic trimers, with the mechanism reviewed elsewhere (53). Carbon loss to gas-phase products was insignificant, with liquid mass balance closure >90% after catalyst filtration. Previous efforts have demonstrated the regenerability of $Nb_2O_5$ for 4-heptanone condensation and recycle of solvent and unreacted ketone (25), with further work needed to evaluate continuous reactor configurations and compatible solvent formulations. Enone products were recovered by distillation and processed neat over the same 3 wt% $Pt/Al_2O_3$ hydrodeoxygenation catalyst (*SI Appendix*, Fig. S10). The recovered hydrocarbon phase was used for testing without further workup.

The neat Aldol Condensation VFA-SAF showed a higher average carbon number of 13.8 due to the coupling step that converts $C_5$ to $C_7$ ketones into predominantly $C_{10}$ to $C_{14}$ enones (Fig. 4*D*). The sample contained 76% isoparaffins, with 13% normal paraffins, 9% monocycloparaffins, and 1% aromatics, with ring structures likely due to trimer formation during ketone condensation (38, 53, 54). The relatively low percentage of ≤C10 hydrocarbons resulted in a higher flash point of 62 °C compared to Jet A, while the high degree of branching resulted in a freezing point of −53 °C comparable to Jet A, despite the higher average carbon number. However, the isoparaffin branching resulted in low temperature viscosity at −40 °C being out of spec (24 cSt, spec max 12 cSt), with a strong temperature dependence relative to the Fast Track VFA-SAF and Jet A (*SI Appendix*, Fig. S11). Future work may address this limitation by fractionating $\geq C_{17}$ hydrocarbons for renewable diesel fuel applications. It is worth noting that the neat Aldol Condensation VFA sample displays advantageous diesel fuel properties (55) with an exceptionally high cetane number of 73 and energy density of 44.41 MJ/kg, similar to HEFA diesel (*SI Appendix*, Table S11). This may provide process flexibility for VFA biofuels based on fuel market demand.

Fuel property tests (Table 3) determined an upper blend limit of 30 vol% for Aldol Condensation VFA-SAF, with viscosity at −40 °C as the limiting fuel property. The higher carbon number distribution increased the boiling point distribution upon blending with Jet A, while the blend's flashpoint of 53 °C was within the typical range of fossil jet. Freezing point was modestly improved to −53 °C, while specific energy density increased to 43.4 MJ/kg that was above the typical range of fossil jet. Normalized sooting concentration of the 30 vol% blend was reduced by 15% relative to fossil Jet A.

**Coblending VFA-SAF.** Synergistic blending was then evaluated by combining Fast Track and Aldol Condensation VFA-SAF due to their complementary limiting fuel properties. Samples were produced from the same $C_4/C_6$ VFA starting material using ketones $\geq C_8$ for Fast Track and ketones $<C_8$ for Aldol Condensation. Since flashpoint is typically dictated by the lowest boiling components in the mixture, a 20 vol% blend limit was maintained for Fast Track VFA-SAF (*SI Appendix*, Tables S8 and S9). In contrast, viscosity is a function of the overall hydrocarbon mixture composition; therefore, it was reasoned that the low-viscosity Fast Track normal paraffins would offset the high-viscosity Aldol Condensation isoparaffins.

As shown in Fig. 4 *G–I*, coblending normal 20 vol% Fast Track VFA-SAF increased the blend limit of Aldol Condensation VFA-SAF from 30 vol% to 50 vol%, resulting in an overall VFA-SAF content of 70 vol%. Fuel property measurements (Table 3) determined the 70 vol% blend displayed a reduced freezing point of −61 °C and significantly increased energy density of 43.7 MJ/kg, well above the typical range for fossil jet. The high energy density of neat $C_4/C_6$ Fast Track and $C_4/C_6$ Aldol Condensation VFA-SAF, at 44.49 and 44.1 MJ/kg, respectively, is comparable to HEFA SAF, Fischer Tropsch SPK, and alcohol-to-jet (*SI Appendix*, Table S7) (56, 57). The high energy density can provide petroleum refiners with the ability to blend VFA-SAF into lower energy density distillates, potentially motivating adoption. Normalized soot concentration also decreased by 34% upon blending, consistent with the blend's reduced aromatic content of 5.8%. Although the accepted low limit for aromatic compounds is 8%, a recent study indicates that cycloalkanes can replace aromatics in terms of volume swell. The combination of 5.8% aromatic and 16% cycloparaffins may be sufficient to remain above the minimum currently required for polymer seal swell (58), although further work is needed to test VFA-SAF. Cetane number of the blend increased well above the range of conventional jet fuel (CN of 64), while surface tension decreased below the typical range. The latter may have positive implications on ignition quality due to improved (decreased droplet size) fuel spray properties (59).

**Techno-Economic Analysis.** Preliminary techno-economic analysis identified the catalytic process cost drivers to guide future research for VFA-SAF upgrading. The Fast Track VFA-SAF pathway was chosen due to the higher technology and fuel readiness level relative to the Aldol Condensation pathway, since the former employs catalytic packed bed reactors for both ketonization and hydrodeoxygenation. Previous techno-economic analysis work on the aldol condensation pathway can be found elsewhere which focuses on butyric acid from corn stover hydrolysate sugar fermentation (60). The baseline process model scenario (Fig. 5*A*) considered the upgrading process in isolation and utilized a VFA profile corresponding to the $C_4/C_6$ sample as the starting feedstock (carbon distribution in *SI Appendix*, Table S3), as shorter chain VFAs are currently accessible from a wider array of waste

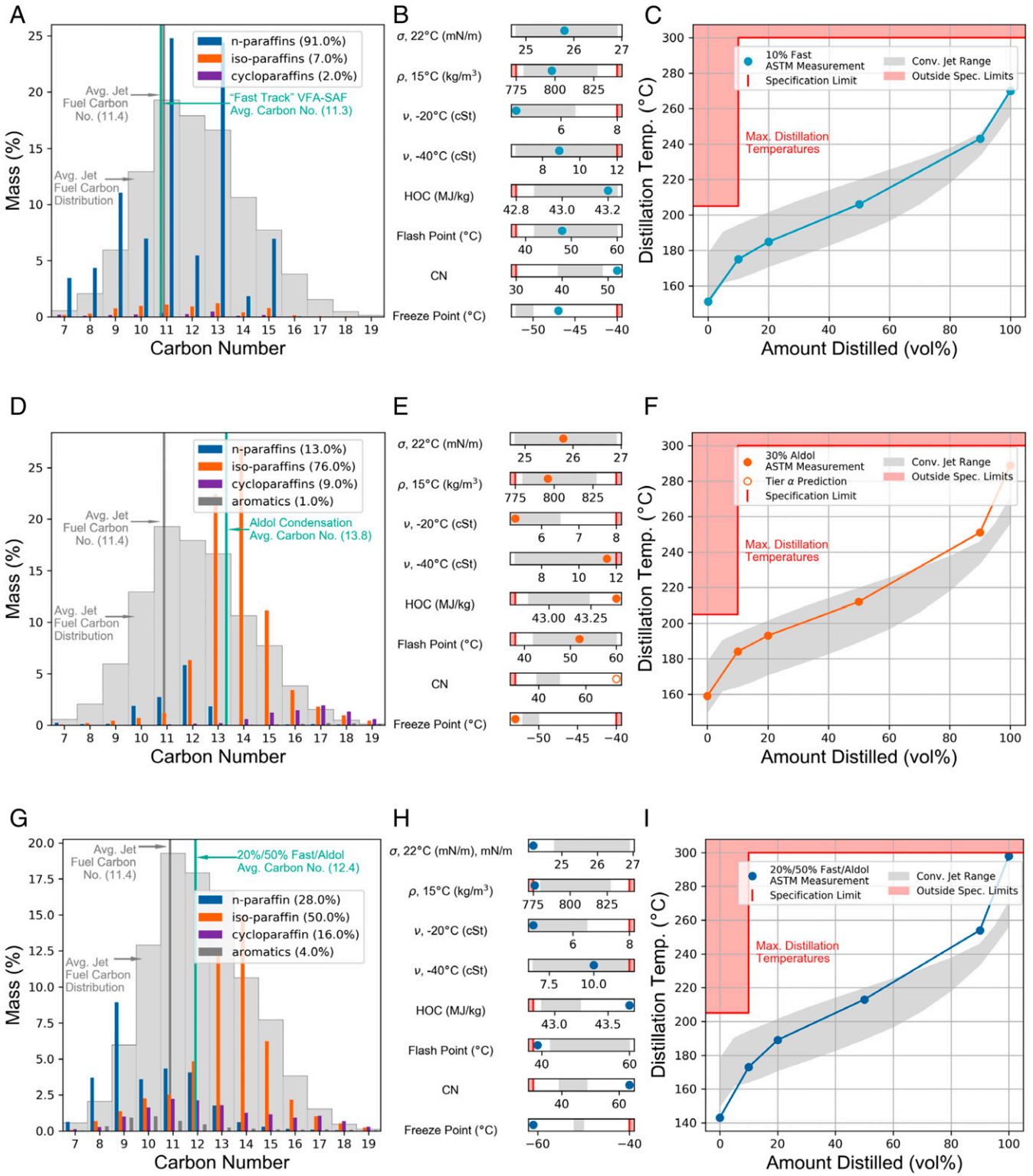


**Fig. 4.** VFA-SAF fuel properties relative to fossil Jet A are shown, prescreened for composition, chemical and physical properties, and distillation analysis. The first row shows Fast Track VFA-SAF blend produced from the $C_6/C_8$ VFA sample (*A*) neat carbon distribution, (*B*) 10 vol% blend fuel properties ($\sigma$ = surface tension, $\rho$ = density, $\mu$ = viscosity, nHOC = net heat of combustion, and CN = cetane number), and (*C*) 10 vol% blend simulated distillation curves. Equivalent data are shown for the Aldol Condensation VFA-SAF produced from the $C_4/C_6$ VFA sample (*D–F*). The 20%/50% Fast Track/Aldol Condensation blend result is shown for all three of its panels (*G–I*). The gray region represents the range of conventional fuels, namely, POSFs 10325, 10264, and 10289. The red regions represent out-of-specification ranges. The carbon distribution for representative fossil jet POSF 10325 is tabulated in *SI Appendix*, Table S6, with fuel properties in *SI Appendix*, Table S8. Predicted data are shown with an open circle.

**Table 3. Measured fuel properties for the 10 vol% Fast Track VFA-SAF blend produced from the $C_6/C_8$ VFA sample, 30 vol% Aldol Condensation VFA-SAF blend produced from the $C_4/C_6$ VFA sample, and 20%/50% Fast Track/Aldol Condensation VFA-SAF blend produced from the $C_4/C_6$ sample**

| Fuel property | Blend criteria (D7566 Table 1) | Jet A POSF 10325 | 10% $C_6/C_8$ Fast track VFA-SAF | 30% $C_4/C_6$ Aldol cond. VFA-SAF | 70% coblending VFA-SAF* |
|---|---|---|---|---|---|
| VFA sample | NA | NA | $C_6/C_8$ | $C_4/C_6$ | $C_4/C_6$ |
| Acidity (mg KOH/g) | Max 0.10 | 0.005 | *0.02* | ND | 0.10 |
| Aromatics (%) | Max 25 | 18 | 16.2 | 12.9 | 5.8 |
| Sulfur (ppm) | Max 3 | 421 | ND | ND | ND |
| T10 | Max 205 | 177 | 175 | 184 | 189 |
| T50 | Report | 205 | 206 | 212 | 213 |
| T90 | Report | 245 | 243 | 251 | 254 |
| T100 | Max 300 | 271 | 270 | 289 | 277 |
| Flash point (°C) | Min 38 | 48 | 48 | 53 | 39 |
| Density, 15 °C (kg/m$^3$) | 775–840 | 802 | 798 | 796 | 776 |
| Freeze point (°C) | Max −40 | −52 | −47 | −53 | −61 |
| Viscosity, −20 °C (mm$^2$/s) | Max 8.0 | 4.7 | 4.4 | 5.2 | 4.6 |
| Viscosity, −40 °C (mm$^2$/s) | Max 12 | 9.6 | 8.9 | 11.5 | 10.0 |
| Surface tension, 22 °C (mN/m) | NA | 24.8 | 25.8 | 25.8 | 24.2 |
| nHOC (MJ/kg) | Min 42.8 | 43.0 | 43.2 | 43.4 | 43.7 |
| Indicated cetane number | NA | 48 | 52 | ND | 64 |
| Normalized soot concentration | NA | 1 | *0.94* | 0.85 | 0.66 |

Values are provided for D7566 specs and fossil Jet A. Volume percent closure for blends is with fossil Jet A. ND: not determined experimentally due to volume limitations. Italics indicate estimation based on neat measurement. NA: not applicable. Max: maximum. Min: minimum.
*20%/50% $C_4/C_6$ Fast Track/Aldol Condensation VFA-SAF Blend in Jet A.

feedstocks and microbial consortia (22, 61, 62). Consistent with the VFA samples evaluated in this work, VFAs were assumed to be recovered neat from fermentation media in their nonsalt form with no additional pretreatment steps required. The VFA upgrading plant scale was based on an assumed food waste availability of 225 wet tons per day and a yield of 0.45 kg VFA/kg dry food waste. VFA ketonization yields were based on experimental results with the full suite of ketones sent for hydrodeoxygenation. Ketones $\leq C_7$ were converted to naphtha suitable for gasoline applications. This resulted in a VFA catalytic upgrading plant capacity of 2.17 MGPY of VFA yielding 1.63 MGPY of liquid hydrocarbon biofuel (gasoline gallon equivalent energy basis). Further information on the techno-economic model and assumptions can be found in *SI Appendix*.

The carbon yield of VFA to fuel for the upgrading process was 85%, with 46% carbon yield to SAF and 39% to naphtha; carbon losses are attributed to the $CO_2$ produced in the ketonization reactions and ketones lost with the aqueous phase during separation. This compares favorably to the estimated HEFA-SAF carbon yield with lipids to fuel of ∼89% (34% SAF, 50% renewable diesel, and 5% naphtha) (11). Conversely, the upstream yield of 0.45 kg VFA/kg dry food waste corresponded to an estimated carbon yield of 56%. The higher yield losses observed in the upstream food waste conversion process are mainly attributed to the $CO_2$ and digestate resulting from anaerobic digestion. Considering the full process of food waste to fuel, an overall carbon yield of 48% was observed, with VFA-SAF and naphtha carbon yields of 26% and 22%, respectively. Further work is needed to evaluate overall process yields with additional wet waste feedstocks (e.g., manure and wastewater sludge).

With VFA production still in the early stages of development and commercialization, the cost of VFA biofuel was evaluated as a function of VFA selling price (Fig. 5*B*). VFA production costs are highly dependent on variables such as the food waste composition, anaerobic digestion process parameters, separation technology, and potential to sell a portion of VFAs into chemical markets. Research is ongoing to advance upstream VFA fermentation and separation technology to reduce process costs and enable the use of diverse wet waste feedstocks (14, 22, 29–31); therefore, techno-economic analysis of upstream VFA production costs was deemed to be outside the scope of this work. At a jet fuel selling price of $2.50/gallon without carbon intensity reduction credits, profitable VFA-SAF production can be realized at a maximum VFA feedstock production cost $1.08/gallon ($0.30/kg). This price point for VFA is comparable to recent lignocellulosic sugar production cost estimates from mixed feedstocks that range from $0.36 to 0.50/kg (61). Recent work has estimated that VFAs could be produced from brown algae via anaerobic digestion and membrane distillation at a cost of $0.38/kg (63). Current market prices of VFAs vary by chain length and can range from $0.40 to 2.50/kg (22); however, it should be emphasized that these market prices are based on current (largely fossil-based) production methods for individual VFAs and do not necessarily relate to production cost of mixed VFAs from a feedstock such as food waste.

Single-point sensitivity analysis was then performed on the selected downstream catalytic conversion parameters (Fig. 5*C*). The VFA upgrading process is largely a capital-driven process, with a capital intensity of $5.40 per gasoline gallon equivalent (GGE) of annual plant capacity. Capital estimates done here are a feasibility-level estimate and may vary significantly from actual capital expenditures. To account for this, a contingency of ±50% is applied to the overall installed plant costs. Separately, the same factor is applied to the ketonization and hydrodeoxygenation reactors individually, given that they are the largest equipment cost drivers. A 50% increase in the overall capital costs increases the minimum fuel selling price by 14%, and similar changes to the ketonization and HDO reactor costs results in minimum fuel selling price increases of 5% and 3%, respectively. The sensitivity to income tax rate was also considered, demonstrating a rate of 35% (corresponding to the US corporate tax rate prior to 2018) only resulted in a 2% increase in minimum fuel selling price compared to the base case tax rate of 21%.

The relatively low catalyst requirements of both reactors resulted in the maximum VFA production cost being rather invariant to large changes (±50%) in weight hourly space velocity and single-purchase catalyst material costs. Selectivity through each reaction was shown to have a strong impact when nontarget products were sent to the steam boiler for heat recovery, rather than contributing to biofuel. The high single-purchase cost of the

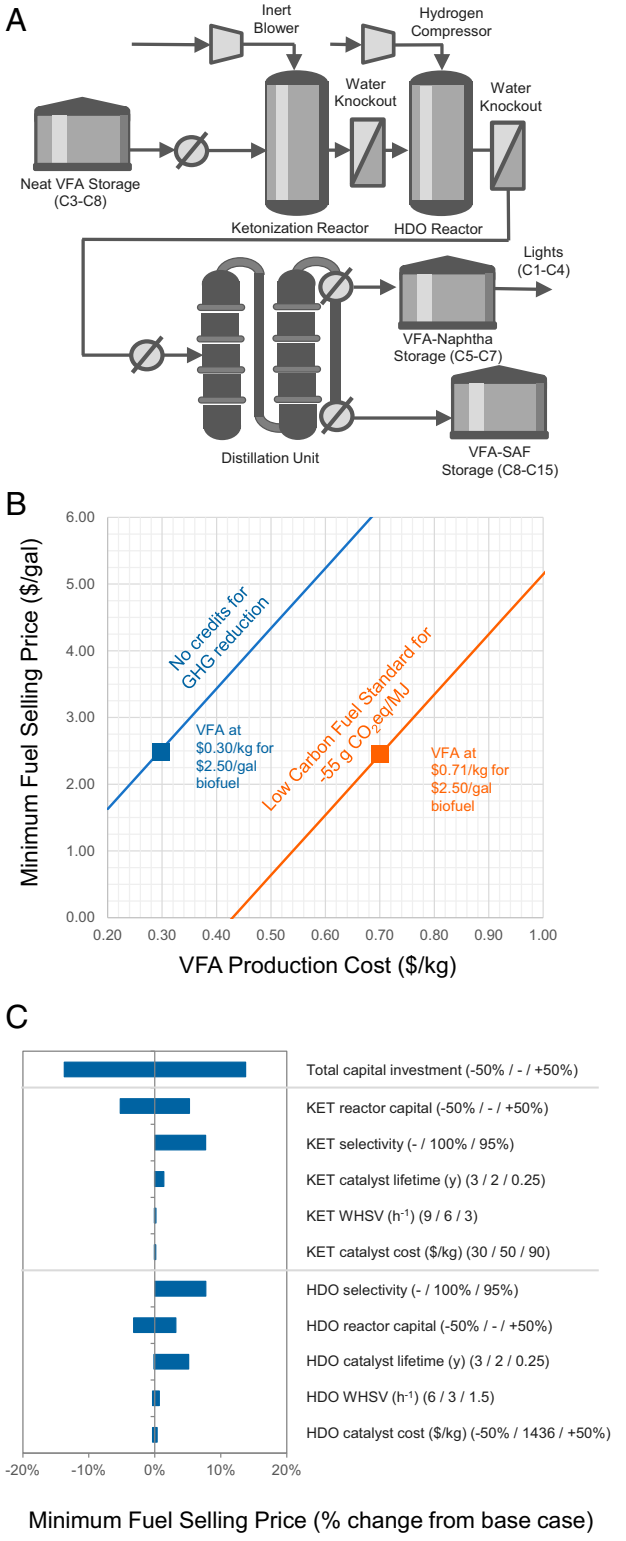


**Fig. 5.** Techno-economic analysis of VFA-SAF Fast Track process. (*A*) Simplified process flow diagram for the downstream catalytic Fast Track VFA-SAF production via ketonization (KET) and hydrodeoxygenation (HDO), with light $\leq C_7$ ketones being converted to naphtha. (*B*) VFA biofuel minimum fuel selling price as a function of VFA production cost and assumed LCFS credit of $3.71/gallon. (*C*) Sensitivity analysis of major downstream catalytic process parameters for VFA biofuel production.

3 wt% $Pt/Al_2O_3$ ($1436/kg) had a measurable effect when considering a material lifetime on the order of months, even when accounting for metal reclamation savings. However, at the base case assumed lifetime of 2 y, impacts of the catalyst cost were minimal. Alternative, low-cost (<$50/kg) HDO catalysts such as those based on Ni or Co have been demonstrated (64); however, we estimate that the impact of switching to one of these base-metal catalysts is on the order of one cent per gallon of VFA with a lifetime of 2 y. As noted above, future studies will evaluate VFA clean-up strategies to further reduce sulfur and other impurities as well as the use of nonprecious catalysts (65–67). The cost of the $ZrO_2$ ketonization catalyst was estimated at $50/kg (68); therefore, even reducing the ketonization catalyst lifetime to 3 mo maintained VFA production costs within 1% of the baseline scenario. This highlights the importance of focusing on catalyst selectivity and, in the case of HDO, lifetime, rather than further optimizing parameters such as weight hourly space velocity.

**Life Cycle Analysis.** The carbon intensity of the VFA-SAF Fast Track process was then evaluated using life cycle analysis. Upstream VFA production and recovery flow rates for life cycle inventory were based on technical consultation with Earth Energy Renewables for this early-stage technology. VFA fermentation and recovery is an emerging technology area, with process flow streams anticipated to vary based on the upstream process technology configuration, waste feedstock composition, technology readiness level, and scale of implementation. VFA catalytic upgrading parameters were based on this study's process model.

The carbon intensity for VFA-SAF was largely driven by avoided methane emissions associated with food waste, with a breakdown of associated $CO_2$ emissions and credits shown in *SI Appendix*, Fig. S12. Diverting food waste from landfills resulted in negative carbon emissions by avoiding methane release (−154 g $CO_2$eq/MJ), while VFA production and VFA catalytic upgrading accounted for 84 g $CO_2$eq/MJ and 15 g $CO_2$eq/MJ in emissions, respectively. This resulted in an overall carbon footprint for Fast Track VFA-SAF of −55 g $CO_2$eq/MJ, which is 165% lower than fossil jet fuel (85 g $CO_2$eq/MJ). Biogenic $CO_2$ emitted from VFA-SAF combustion was accounted for as a credit per life cycle analysis convention (69).

Using California's LCFS credit calculator for renewable diesel, the carbon intensity reduction would provide a credit of $3.71/gallon (70). Assuming the target VFA-SAF minimum full selling price remains fixed at $2.50/gallon, this credit would allow VFA production costs to be no more than $0.71/kg (Fig. 5*B*). Renewable Identification Number credits under the US Environmental Protection Agency (EPA) Renewable Fuel Standard would offer additional economic incentives (71). If the 70% blend limit for VFA-SAF can be achieved with comparable life cycle inputs, the 165% reduction in lifecycle greenhouse gas emissions would provide a path toward net zero jet fuel.

While this preliminary analysis suggests the potential for significant greenhouse gas savings with VFA-SAF, it should be noted that baseline practices for wet waste management will continue to evolve, as will VFA-SAF technology. New legislation in California recently mandated a 75% reduction of landfill organics from 2014 levels by 2025 using alternative disposal practices such as composting and anaerobic digestion (72). Eliminating the avoided methane credit would lead to a carbon intensity increase by 16% compared to fossil jet fuel based on the parameters used for this analysis. Widespread changes to landfill organic waste management would impact the baseline for avoided landfill methane emission credits evaluated here and motivate VFA production from additional wet waste feedstocks including manure, wastewater sludge, algae, and lignocellulosic biomass (14, 22). In addition, advancements in renewable electricity and green hydrogen production stand to reduce the overall carbon footprint of upstream

and downstream VFA-SAF unit operations. Significant potential also exists for carbon sequestration through the land application of biosolids produced during VFA fermentation (73), which was beyond the scope of this study. As such, several long-term opportunities exist to advance VAF-SAF toward net-zero emissions as the technology develops with cost and carbon footprint targets in mind.

## Conclusion

This work demonstrates the conversion of food waste–derived VFAs into SAF consisting of normal paraffins suitable for ASTM Fast Track qualification at 10 vol% blends, as well as highly branched isoparaffins produced via aldol condensation that can offer increased blending while maintaining ASTM fuel property specs. Statistical distribution models for VFA ketonization identified the VFA carbon chain length distributions suitable for each SAF upgrading pathway with stable ketonization catalyst time on stream performance observed for >100 h and minimal biogenic impurities in the final hydrocarbon fuel. Fuel property testing of the normal paraffin Fast Track VFA-SAF determined that flash point is the limiting fuel property, with a 20 vol% blend limit. Conversely, low-temperature viscosity was the limiting fuel property with Aldol Condensation VFA-SAF, with a 30 vol% blend limit. Due to their complementary fuel property limitations, synergistic blending was observed when combining Fast Track and Aldol Condensation of VFA-SAF to increase the overall blend limit to 70 vol%. Techno-economic analysis for VFA catalyst upgrading determined VFAs can be produced at $0.30/kg to achieve a Fast Track minimum fuel selling price of $2.50/gallon. Due to the potential for significant avoided methane emissions when diverting food waste from landfills for VFA production, life cycle analysis determined that VFA-SAF has potential to provide up to 165% reduction in greenhouse gas emissions relative to fossil jet fuel.

## Materials and Methods

A brief description of the materials and methods is provided here, with additional details found in *SI Appendix*.

**VFA Feedstock.** VFA samples were provided by Earth Energy Renewables in their neat form following anaerobic digestion of food waste and recovery from fermentation media. Inorganic impurities were measured using inductively coupled plasma mass spectroscopy. Model VFAs for ketonization catalyst stability testing were obtained from Sigma-Aldrich.

**Ketonization Kinetic Model.** A simplified kinetic model was used to predict ketone profiles at 100% conversion of VFAs. Equations were solved using MATLAB software.

**Catalytic Upgrading.** VFAs were catalytically upgraded via ketonization over $ZrO_2$ in a custom-built flow reactor that was outfitted with an online NDIR detector. Spinning band distillation was performed to separate ketones $\geq C_8$ from those $\leq C_7$. Aldol condensation was performed on ketones $\leq C_7$ using a glass Dean–Stark reactor system with $Nb_2O_5$. Solvent and unreacted ketones were removed from the resulting enones by spinning band distillation. Hydrodeoxygenation was performed in the custom-built flow reactor over $Pt/Al_2O_3$ for the neat $\geq C_8$ ketone sample as well as the neat enone sample. Products were analyzed with a GC equipped with a Polyarc flame ionization detector and mass spectrometer.

**Catalyst Characterization.** $ZrO_2$ catalyst used for VFA ketonization was analyzed by physisorption, $NH_3$ temperature–programmed desorption, pyridine diffuse reflectance Fourier transform infrared spectroscopy, TGA, CHN, STEM-EDS, and XPS.

**Fuel Property Analysis.** Hydrocarbon analysis was performed by GCxGC, and distillation behavior was analyzed by GC. VFA-SAF fuel properties were estimated and measured using Tier $\alpha$ and $\beta$ testing along with additional ASTM measurements conducted for the net heat of combustion, percent hydrogen, acid content, and nitrogen content. Sooting tendency was measured by yield sooting index.

**Techno-Economic Analysis and Life Cycle Analysis.** The process model was developed in Aspen Plus to determine the mass and energy balance. Model outputs were used for financial analysis. Catalyst costs were estimated using CatCost (68). Life cycle analysis was performed using data from GREET (74), SimaPro (75), and literature.

**Data Availability.** All study data are included in the article and/or *SI Appendix*.

**ACKNOWLEDGMENTS.** We would like to acknowledge Cesar Granda and the employees of Earth Energy Renewables for providing VFA samples for catalytic upgrading. We thank S.K. Reeves for assistance with transmission electron microscopy sample preparation, Wilson McNeary for sulfur poisoning research and advising, Jacob Miller for catalyst testing experimental support, and Joel Miscall, Jon Luecke, and Gina Fioroni for valuable fuel property measurement and strategic discussions. We thank also Amma O. Kankam for sooting measurements and Lisa D. Pfefferle for useful discussion surrounding soot and emissions as well as Eric Karp for his review and feedback on VFA separations. A portion of this research was conducted as part of the Opportunities in Biojet Project sponsored by the US Department of Energy Office of Energy Efficiency and Renewable Energy and Bioenergy Technologies (BETO) and Vehicle Technologies Offices at the National Renewable Energy Laboratory (NREL) through Contract No. DE-AC36-08GO28308. A portion of this work was also conducted as part of the Chemical Catalysis for Bioenergy Consortium sponsored by BETO through Contract No. DE-AC36-08GO28308 at NREL. Diesel fuel property testing for VFA hydrocarbons was supported by the Co-Optimization of Fuels & Engines (Co-Optima) project sponsored by the US Department of Energy - Office of Energy Efficiency and Renewable Energy and BETO and Vehicle Technologies Offices at NREL through Contract No. DE347AC36-99GO10337. Microscopy was performed in collaboration with the Chemical Catalysis for Bioenergy Consortium under Contract No. DE-AC05-00OR22725 with Oak Ridge National Laboratory (ORNL) and through a user project supported by ORNL's Center for Nanophase Materials Sciences, which is sponsored by the Scientific User Facilities Division, Office of Basic Energy Sciences, US Department of Energy. Part of the microscopy research was also supported by the Office of Nuclear Energy, Fuel Cycle Research & Development Program, and the Nuclear Science User Facilities. Work at the University of Dayton was supported by BETO through subcontract PO 2196073. Work at Yale was supported by the Co-Optima project sponsored by BETO through Contract No. DE-EE0008726. The views expressed in the article do not necessarily represent the views of the US Department of Energy or the US Government. The US Government retains and the publisher, by accepting the article for publication, acknowledges that the US Government retains a nonexclusive, paid-up, irrevocable, worldwide license to publish or reproduce the published form of this work, or allow others to do so, for US Government purposes.

1. J. Holladay, Z. Abdullah, J. Heyne, "Sustainable aviation fuel: Review of technical pathways" (DOE/EE-2041 8292, USDOE Office of Energy Efficiency and Renewable Energy (EERE), Bioenergy Technologies Office (EE-3B) (Bioenergy Technologies Office Corporate), DOE EERE, 2020).
2. ICAO, Assembly Resolutions in Force. https://www.icao.int/Meetings/GLADs-2015/Documents/A38-18.pdf. Accessed 1 March 2021.
3. D. S. Lee *et al*., The contribution of global aviation to anthropogenic climate forcing for 2000 to 2018. *Atmos. Environ. (1994)* **244**, 117834 (2021).
4. ICAO, Resolutions Adopted by the Assembly: Provisional Edition. 38th Session, Montreal, Canada. September 24 - October 13 (2013).
5. L. Zhang, T. L. Butler, B. Yang, *Recent Trends, Opportunities and Challenges of Sustainable Aviation Fuel* (Green Energy to Sustainability, 2020), pp. 85–110.
6. Airlines.org, Airlines for America, Airlines Fly Green. (2020). https://www.airlines.org/airlines-fly-green/. Accessed 30 October 2020.
7. R. H. Moore *et al*., Biofuel blending reduces particle emissions from aircraft engines at cruise conditions. *Nature* **543**, 411–415 (2017).
8. B. Kärcher, Formation and radiative forcing of contrail cirrus. *Nat. Commun.* **9**, 1824 (2018).
9. IRENA, *Biofuels for Aviation: Technology Brief* (International Renewable Energy Agency, Abu Dhabi, 2017).
10. US-EIA, *"U.S. energy information administration, annual energy outlook 2020 with projections to 2050" EPA 456-R-21-001* (US Department of Energy, Office of Energy Analysis, 2020).
11. M. Pearlson, C. Wollersheim, J. Hileman, A techno-economic review of hydroprocessed renewable esters and fatty acids for jet fuel production. *Biofuels Bioprod. Biorefin.* **7**, 89–96 (2013).
12. D. Scheitrum, Impact of intensity standards on alternative fuel adoption: Renewable natural gas and California's low carbon fuel standard. *Energy J.* **41**, 191–218 (2020).
13. M. M. Bomgardner, *California refiners shift production to renewable diesel. C&EN* (American Chemical Society, 2020), vol. 98.
14. A. H. Bhatt, Z. J. Ren, L. Tao, Value proposition of untapped wet wastes: Carboxylic acid production through anaerobic digestion. *iScience* **23**, 101221 (2020).

15. R. L. Skaggs, A. M. Coleman, T. E. Seiple, A. R. Milbrandt, Waste-to-Energy biofuel production potential for selected feedstocks in the conterminous United States. *Renew. Sustain. Energy Rev.* **82**, 2640–2651 (2018).
16. US-EPA, *Documentation chapters for GHG emissions and energy factors used in the waste reduction model* (Environmental Protection Agency, 2019).
17. U. Lee, J. Han, M. Wang, Evaluation of landfill gas emissions from municipal solid waste landfills for the life-cycle analysis of waste-to-energy pathways. *J. Clean. Prod.* **166**, 335–342 (2017).
18. J. Poore, T. Nemecek, Reducing food's environmental impacts through producers and consumers. *Science* **360**, 987–992 (2018).
19. US-BETO, "Biofuels and bioproducts from wet and gaseous waste streams: Challenges and opportunities" (DOE/EE 1472 7601, OSTI, 2017).
20. C. Mao, Y. Feng, X. Wang, G. Ren, Review on research achievements of biogas from anaerobic digestion. *Renew. Sustain. Energy Rev.* **45**, 540–555 (2015).
21. US-EPA, An overview of renewable natural gas from biogas (EPA 456-R-20-001, EPA, 2020).
22. M. Atasoy, I. Owusu-Agyeman, E. Plaza, Z. Cetecioglu, Bio-based volatile fatty acid production and recovery from waste streams: Current status and future challenges. *Bioresour. Technol.* **268**, 773–786 (2018).
23. G. R. Hafenstine *et al*., Single-phase catalysis for reductive etherification of diesel bioblendstocks. *Green Chem.* **22**, 4463–4472 (2020).
24. M. T. Holtzapple *et al*., Biomass conversion to mixed alcohol fuels using the MixAlco process. *Appl. Biochem. Biotechnol.* **77-79**, 609–631 (1999).
25. X. Huo *et al*., Tailoring diesel bioblendstock from integrated catalytic upgrading of carboxylic acids: A "fuel property first" approach. *Green Chem.* **21**, 5813–5827 (2019).
26. N. A. Huq *et al*., Performance-advantaged ether diesel bioblendstock production by a priori design. *Proc. Natl. Acad. Sci. U.S.A.* **116**, 26421 (2019).
27. M. Amer *et al*., Low carbon strategies for sustainable bio-alkane gas production and renewable energy. *Energy Environ. Sci.* **13**, 1818–1831 (2020).
28. E. A. Tampio, L. Blasco, M. M. Vainio, M. M. Kahala, S. E. Rasi, Volatile fatty acids (VFAs) and methane from food waste and cow slurry: Comparison of biogas and VFA fermentation processes. *Glob. Change Biol. Bioenergy* **11**, 72–84 (2019).
29. M. Venkateswar Reddy, G. Kumar, G. Mohanakrishna, S. Shobana, R. I. Al-Raoush, Review on the production of medium and small chain fatty acids through waste valorization and $CO_2$ fixation. *Bioresour. Technol.* **309**, 123400 (2020).
30. R. S. Nelson, D. J. Peterson, E. M. Karp, G. T. Beckham, D. Salvachúa, Mixed carboxylic acid production by megasphaera elsdenii from glucose and lignocellulosic hydrolysate. *Fermentation (Basel)* **3**, 10 (2017).
31. P. O. Saboe *et al*., In situ recovery of bio-based carboxylic acids. *Green Chem.* **20**, 1791–1804 (2018).
32. D. M. Alonso, J. Q. Bond, J. C. Serrano-Ruiz, J. A. Dumesic, Production of liquid hydrocarbon transportation fuels by oligomerization of biomass-derived C9 alkenes. *Green Chem.* **12**, 992–999 (2010).
33. E. V. Fufachev, B. M. Weckhuysen, P. C. A. Bruijnincx, Tandem catalytic aromatization of volatile fatty acids. *Green Chem.* **22**, 3229–3238 (2020).
34. B. G. Harvey, H. A. Meylemans, 1-Hexene: A renewable C6 platform for full-performance jet and diesel fuels. *Green Chem.* **16**, 770–776 (2014).
35. V. Vorotnikov *et al*., Inverse bimetallic RuSn catalyst for selective carboxylic acid reduction. *ACS Catal.* **9**, 11350–11359 (2019).
36. B. Boekaerts, B. F. Sels, Catalytic advancements in carboxylic acid ketonization and its perspectives on biomass valorisation. *Appl. Catal. B* **283**, 119607 (2020).
37. T. N. Pham, T. Sooknoi, S. P. Crossley, D. E. Resasco, Ketonization of carboxylic acids: Mechanisms, catalysts, and implications for biomass conversion. *ACS Catal.* **3**, 2456–2473 (2013).
38. S. Shylesh *et al*., Integrated catalytic sequences for catalytic upgrading of bio-derived carboxylic acids to fuels, lubricants and chemical feedstocks. *Sustain. Energy Fuels* **1**, 1805–1809 (2017).
39. ASTM D7566 (20b), "Standard specification for aviation turbine fuel containing synthesized hydrocarbons" (D7566 - 20c, ASTM International, West Conshohocken, PA, 2020).
40. J. S. Heyne *et al*., "Year 2 of the National jet fuels combustion program: Towards a streamlined alternative jet fuels certification process" in *55th AIAA Aerospace Sciences Meeting, AIAA SciTech Forum* (American Institute of Aeronautics and Astronautics, 2017).
41. ASTM D4054 (20c), "Standard practice for evaluation of new aviation turbine fuels and fuel additives" (D4054 - 20c, ASTM International, West Conshohocken, PA, 2020).
42. J. Hileman, M. Rumizen, "Fuel approval process & status" (slideshow). ICAO environment. Stocktaking seminar: Towards the 2050 vision for sustainable aviation fuels (2019). https://www.icao.int/Meetings/SAFStocktaking/Documents/ICAO%20SAF%20Stocktaking%202019%20-%20AI1-1%20Jim%20Hileman.pdf. Accessed 1 March 2021.
43. M. Colket *et al*., Overview of the national jet fuels combustion Program. *AIAA J.* **55**, 1087–1104 (2017).
44. J. Heyne, B. Rauch, P. LeClercq, M. Colket, Sustainable aviation fuel prescreening tools and procedures. *Fuel* **290**, 120004 (2021).
45. ASTM D1322, "Standard test method for smoke point of Kerosene and aviation turbine fuel (D1322-19, ASTM International, West Conshohocken, PA, 2019).
46. D. D. Das *et al*., Sooting tendencies of diesel fuels, jet fuels, and their surrogates in diffusion flames. *Fuel* **197**, 445–458 (2017).
47. C. A. Gaertner, J. C. Serrano-Ruiz, D. J. Braden, J. A. Dumesic, Ketonization reactions of carboxylic acids and esters over Ceria–Zirconia as biomass-upgrading processes. *Ind. Eng. Chem. Res.* **49**, 6027–6033 (2010).
48. K. Takanabe, K.-i. Aika, K. Seshan, L. Lefferts, Catalyst deactivation during steam reforming of acetic acid over Pt/ZrO2. *Chem. Eng. J.* **120**, 133–137 (2006).
49. X. Du, G. Yang, Y. Chen, J. Ran, L. Zhang, The different poisoning behaviors of various alkali metal containing compounds on SCR catalyst. *Appl. Surf. Sci.* **392**, 162–168 (2017).
50. J. Due-Hansen, A. L. Kustov, S. B. Rasmussen, R. Fehrmann, C. H. Christensen, Tungstated zirconia as promising carrier for DeNOX catalysts with improved resistance towards alkali poisoning. *Appl. Catal. B* **66**, 161–167 (2006).
51. T. Edwards, "Reference jet fuels for combustion testing" in 55th AIAA Aerospace Sciences Meeting (American Institute of Aeronautics and Astronautics, 2017), pp 1–58.
52. S. Shylesh, L. A. Bettinson, A. Aljahri, M. Head-Gordon, A. T. Bell, Experimental and computational studies of carbon–Carbon bond formation via ketonization and aldol condensation over site-isolated zirconium catalysts. *ACS Catal.* **10**, 4566–4579 (2020).
53. E. R. Sacia *et al*., Highly selective condensation of biomass-derived methyl ketones as a source of aviation fuel. *ChemSusChem* **8**, 1726–1736 (2015).
54. S. Shylesh, A. A. Gokhale, C. R. Ho, A. T. Bell, Novel strategies for the production of fuels, lubricants, and chemicals from biomass. *Acc. Chem. Res.* **50**, 2589–2597 (2017).
55. G. Fioroni *et al*., *Screening of Potential Biomass-Derived Streams as Fuel Blendstocks for Mixing Controlled Compression Ignition Combustion* (SAE International, 2019).
56. T. Lee, A. Oldani, I. M. Anderson, National Alternative Jet Fuels Test Database. https://altjetfuels.illinois.edu/. Accessed 15 May 2020.
57. P. Vozka, D. Vrtiška, P. Šimáček, G. Kilaz, Impact of alternative fuel blending components on fuel composition and properties in blends with jet A. *Energy Fuels* **33**, 3275–3289 (2019).
58. S. Kosir, J. Heyne, J. Graham, A machine learning framework for drop-in volume swell characteristics of sustainable aviation fuel. *Fuel* **274**, 117832 (2020).
59. K. C. Opacich, J. S. Heyne, E. Peiffer, S. D. Stouffer, "Analyzing the relative impact of spray and volatile fuel properties on gas turbine combustor ignition in multiple rig geometries" in *AIAA Scitech 2019 Forum* (American Institute of Aeronautics and Astronautics, 2019).
60. R. E. Davis *et al*., "Process design and economics for the conversion of Lignocellulosic biomass to hydrocarbon fuels and coproducts: 2018 biochemical design case update; Biochemical deconstruction and conversion of biomass to fuels and products via integrated biorefinery pathways" (NREL/TP-5100-71949, NREL, 2018).
61. N. R. Baral, R. Davis, T. H. Bradley, Supply and value chain analysis of mixed biomass feedstock supply system for lignocellulosic sugar production. *Biofuels Bioprod. Biorefin.* **13**, 635–659 (2019).
62. B. S. Jeon, O. Choi, Y. Um, B.-I. Sang, Production of medium-chain carboxylic acids by Megasphaera sp. MH with supplemental electron acceptors. *Biotechnol. Biofuels* **9**, 129 (2016).
63. P. Fasahati, J. Liu, "Techno-economic analysis of production and recovery of volatile fatty acids from brown algae using membrane distillation" in *Computer Aided Chemical Engineering*, M. R. Eden, J. D. Siirola, G. P. Towler, Eds. (Elsevier, 2014), vol. 34, pp. 303–308.
64. X. Yang *et al*., Hydrodeoxygenation (HDO) of biomass derived ketones using supported transition metals in a continuous reactor. *ACS Sustainable Chem. Eng.* **7**, 14521–14530 (2019).
65. M. Auersvald *et al*., Quantitative study of straw bio-oil hydrodeoxygenation over a sulfided NiMo catalyst. *ACS Sustainable Chem. Eng.* **7**, 7080–7093 (2019).
66. R. Durand, P. Geneste, C. Moreau, J. L. Pirat, Heterogeneous hydrodeoxygenation of ketones and alcohols on sulfided NiO-MoO3/γ-Al2O3 catalyst. *J. Catal.* **90**, 147–149 (1984).
67. E. Laurent, B. Delmon, Study of the hydrodeoxygenation of carbonyl, carboxylic and guaiacyl groups over sulfided CoMo/γ-Al2O3 and NiMo/γ-Al2O3 catalysts: I. Catalytic reaction schemes. *Appl. Catal. A Gen.* **109**, 77–96 (1994).
68. CatCost, Version 1.0.4, National Renewable Energy Lab (Golden, CO, 2020). https://catcost.chemcatbio.org. Accessed 1 March 2021.
69. J. R. Hannon *et al*., Technoeconomic and life-cycle analysis of single-step catalytic conversion of wet ethanol into fungible fuel blendstocks. *Proc. Natl. Acad. Sci. U.S.A.* **117**, 12576–12583 (2020).
70. CA-EPA, *California EPA Air Resources Board, The LCFS Credit Price Calculator, v1.2* (California Air Resources Board, Sacramento, California, 2017).
71. US-CFR, US Code of Federal Regulations 40 CFR §§ 80.1400–80.1475 (2020).
72. CA-Legislature, California Legislature, SB-1383 Short-lived climate pollutants: methane emissions: Dairy and livestock: Organic waste: Landfills. Chapter 395. §§ 239730.5-39730.7 (2015–2016).
73. G. M. Peters, H. V. Rowley, Environmental comparison of biosolids management systems using life cycle assessment. *Environ. Sci. Technol.* **43**, 2674–2679 (2009).
74. Argonne National Laboratory, Greenhouse gases, regulated emissions, and energy use in technologies (GREET) model. Version 2019 (2019).
75. G Wernet *et al*., The ecoinvent database version 3 (part I): overview and methodology. *Int. J Life Cycle Assess.* **21**, 1218–1230 (2016).